Electronic Supplementary Material (ESI) for ChemComm.

Supporting Information

Fabrication of white luminescence composite films containing Dy-polyoxometalate and study of their luminescence switching behaviors

Wenmei Gao, Tian Yu, Lixin Wu and Lihua Bi

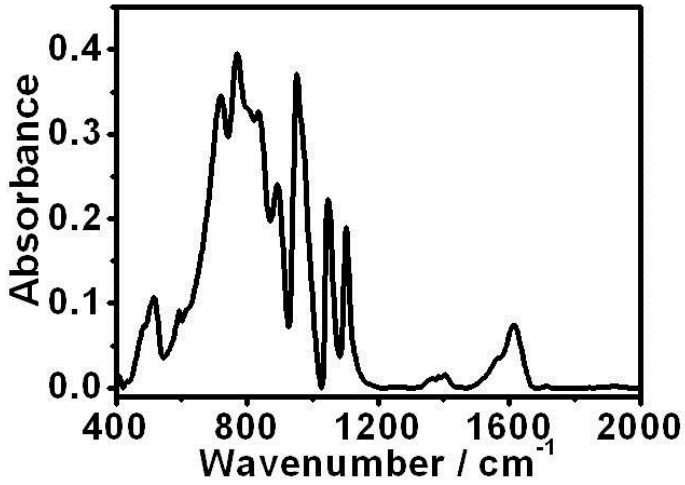

Fig. S1 FT-IR spectrum of DyPW11 in KBr pellet.

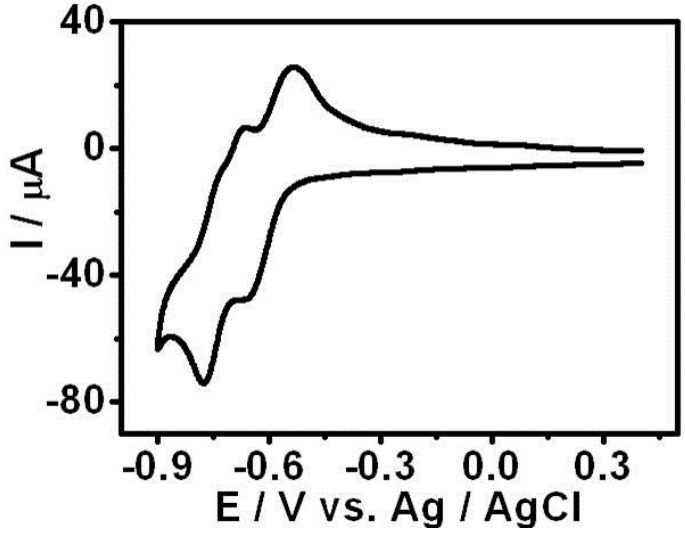

Fig. S2 CV of 1 mM DyPW11 in Na_2SO_4/H_2SO_4 (0.5 M, pH = 2.5) solution at scan rate of 100 mV/s.

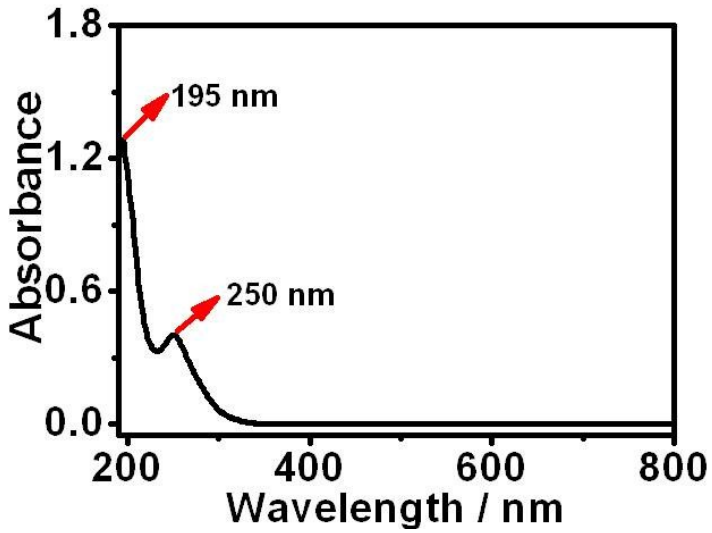

Fig. S3 UV-vis spectrum of 6.5 μM DyPW11 in aqueous solution.

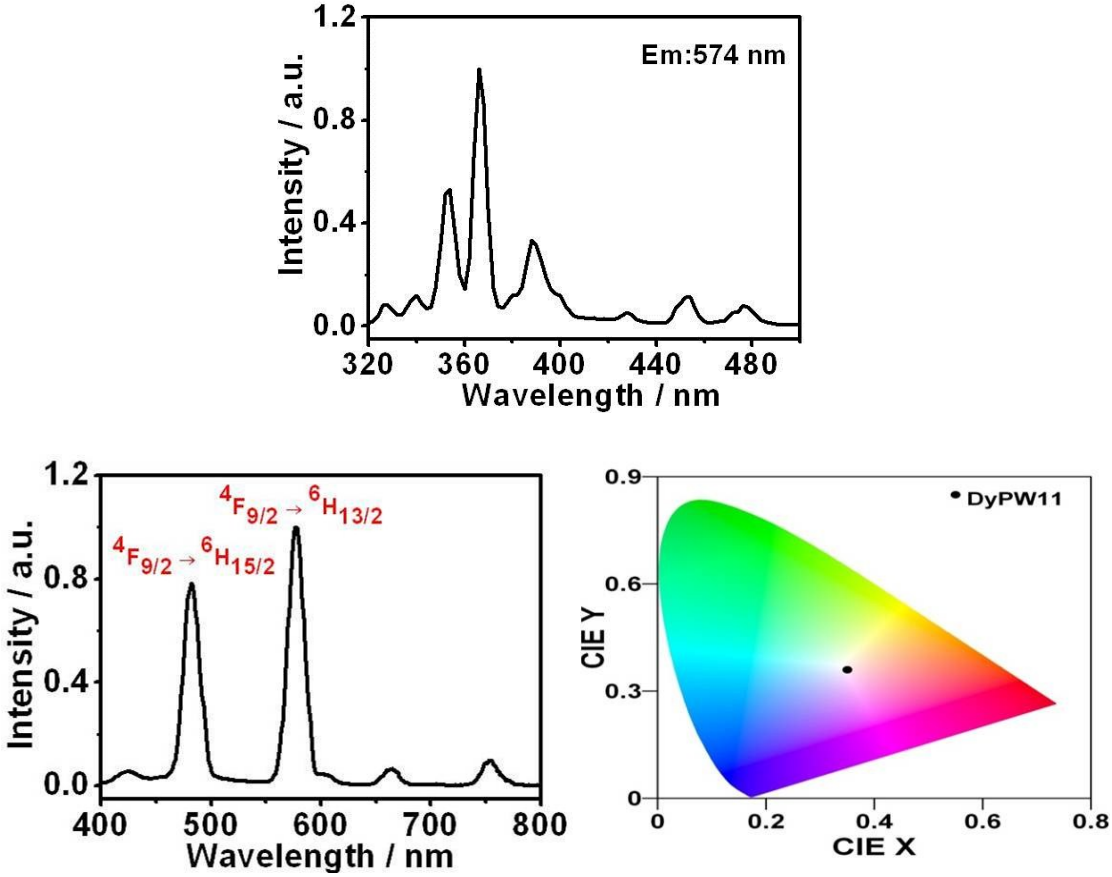

Fig. S4 Normalized excitation spectrum (top) and fluorescence emission spectrum (bottom, left) of 1 mM DyPW11 in aqueous solution and the CIE chromaticity diagram of DyPW11 (bottom, right) excited at 367 nm.

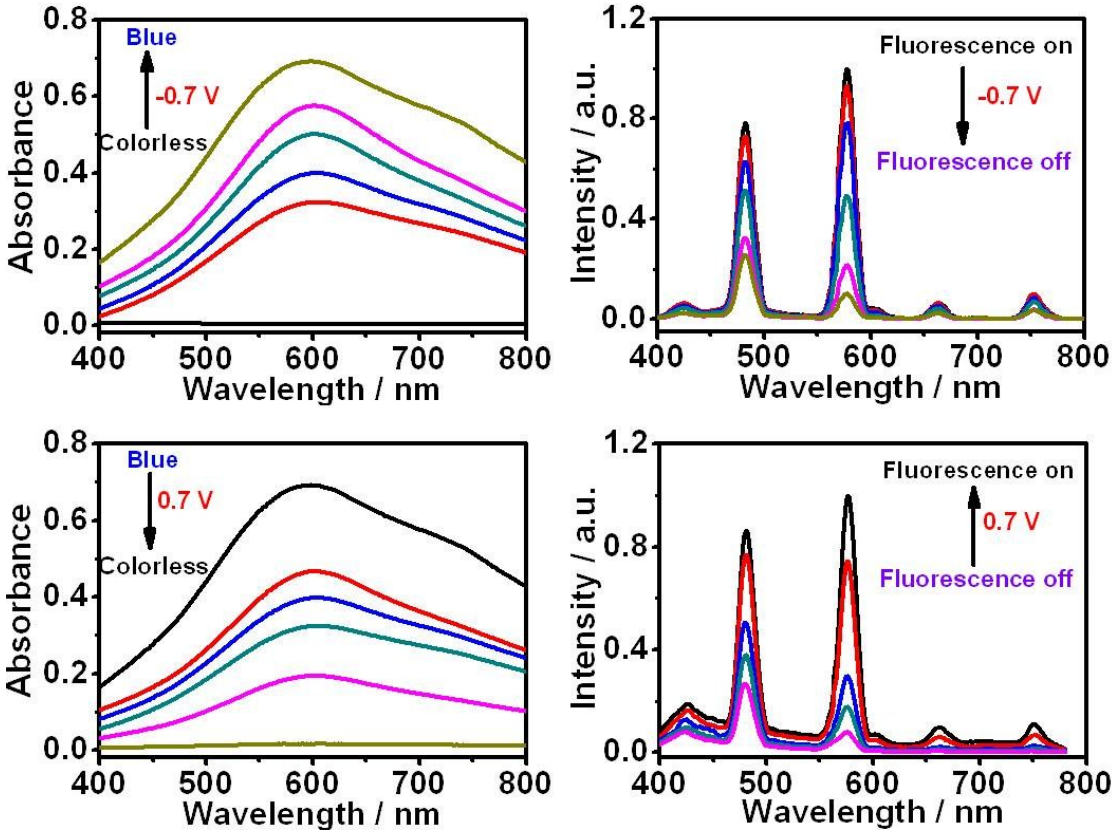

Fig. S5 Changes of visible and normalized fluorescence emission spectra of 1 mM DyPW11 in Na_2SO_4/H_2SO_4 (0.5 M, pH = 2.5) solutions during the redox process of DyPW11 when applied a reduction potential of -0.7 V and an oxidation potential of 0.7 V.

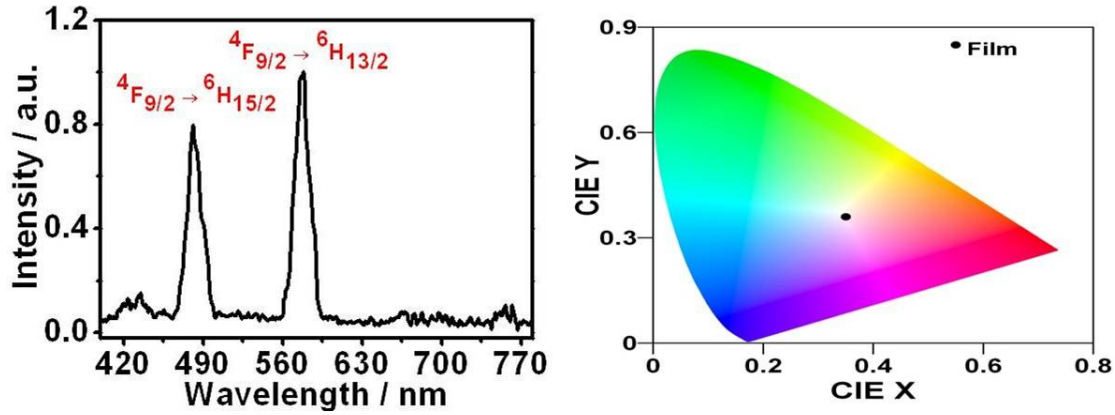

Fig. S6 Normalized fluorescence emission spectrum (left) and the CIE chromaticity diagram of the composite film $(PEI/DyPW11)_{41}$ (right) excited at 367nm.

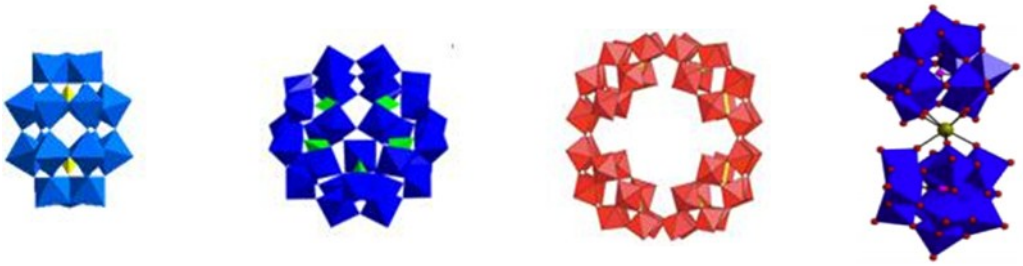

P_2W_{18} P_5W_{30} P_8W_{48} DyPW11

Fig. S7 The polyhedron structures of P_2W_{18}, P_5W_{30}, P_8W_{48} and DyPW11.

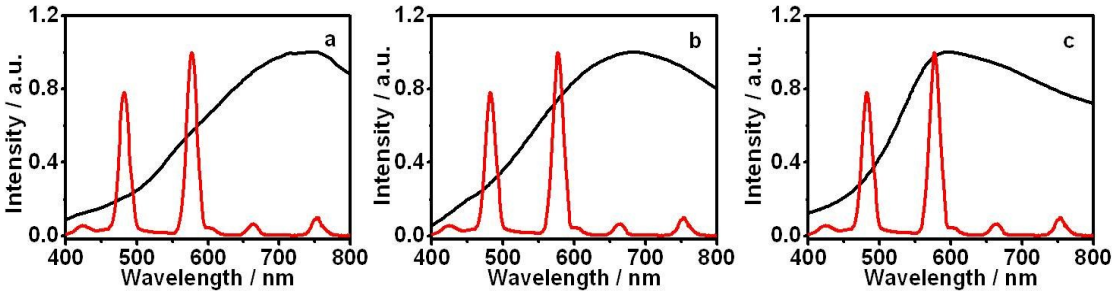

Fig. S8 Overlap graph of normalized luminescence emission spectra (red curve) of 2mM DyPW11 and normalizedVisible spectra(black curve) of the mixture of 2mM DyPW11 and 0.1 mM P_2W_{18}(a), 0.25 mM P_5W_{30}(b), 0.15 mM P_8W_{48} (c) in their electro-reduced state at -0.7 Vin Na_2SO_4/H_2SO_4 (0.5 M, pH = 2.5) solutions.

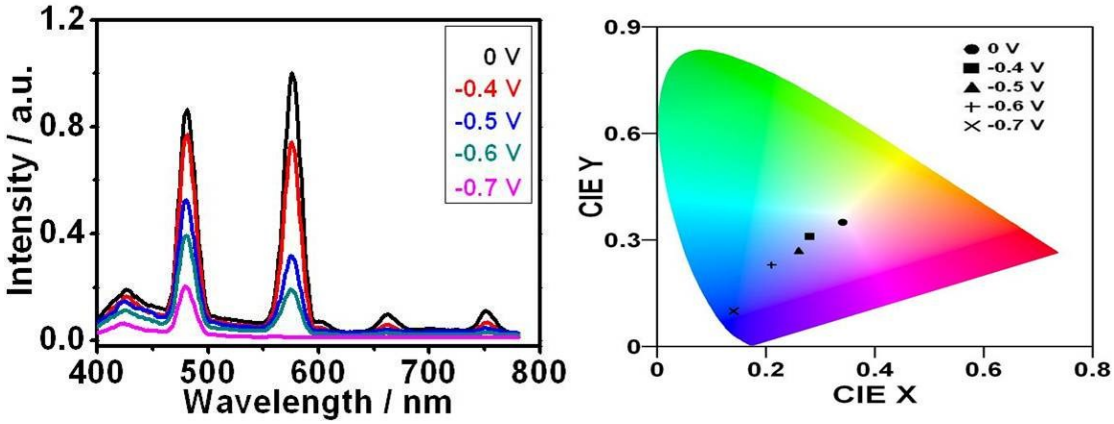

Fig. S9 (Left) Normalized fluorescence emission spectra (λexc = 367 nm) of 2 mM DyPW11 and 1 mM P_8W_{48} in Na_2SO_4/H_2SO_4 (0.5 M, pH 2.5) solution when applied different reduction potentials; (Right) the CIE chromaticity diagram for 2 mM DyPW11 and 1 mM P_8W_{48} in Na_2SO_4/H_2SO_4 (0.5 M, pH 2.5) solution when applied different reduction potentials monitored at 367 nm.

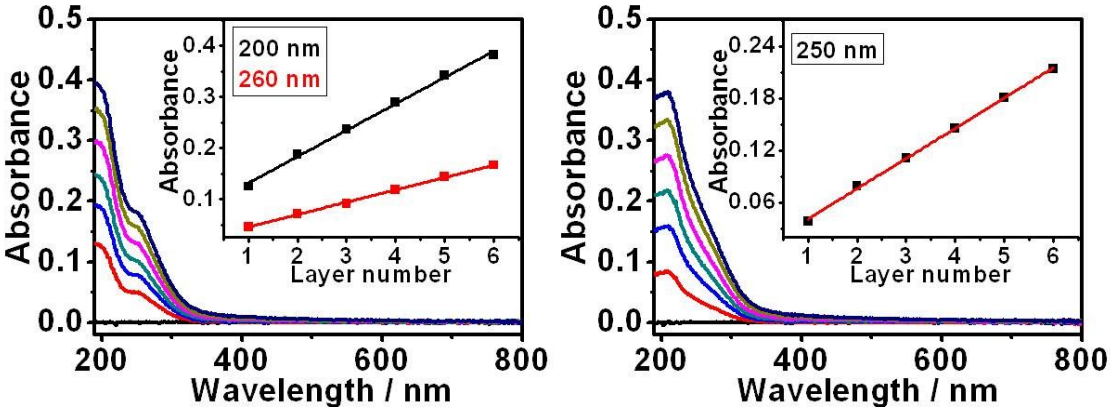

Fig. S10 UV-vis spectra of two composite films $(PEI/DyPW11)_6$ (left) and $(PEI/P_8W_{48})_6$ (right). The insets show the absorbance at 200 nm, 250 nm and 260 nm vs. the number of layers.

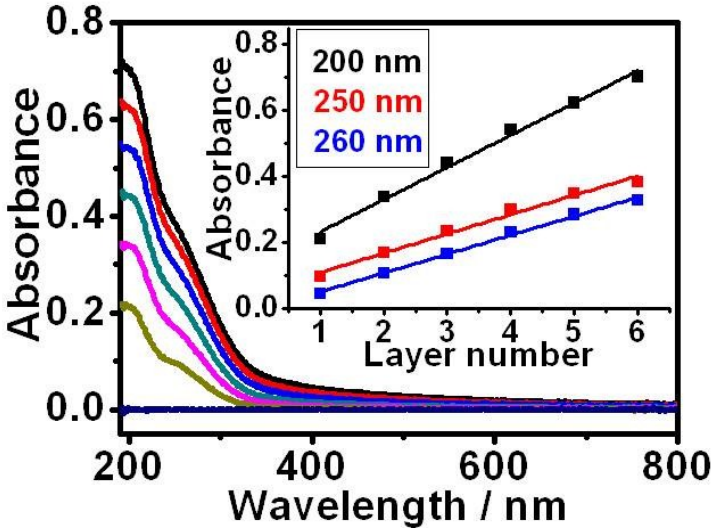

Fig. S11 UV-vis spectra of the composite film $(PEI/P_8W_{48}/PEI/DyPW11)_6$. The inset shows the absorbance at 200 nm, 250 nm and 260 nm vs. the number of layers.

Surface morphology characterization of the composite films

We used atomic force microscopy (AFM) to measure the morphology of two composite films of $(PEI/DyPW11)_1$ and $(PEI/DyPW11)_3$, as shown in Fig. S12-15 below. It can be seen that both films display an almost-spherical granular distribution, which is attributed to the aggregation of DyPW11 in the composite films. This is similar to the other composite films containing polyoxometalates [1]. Moreover, the mean interface roughness values are listed in Table S1 below. It can be observed that the mean interface roughness increases with the layer numbers. The thicker of the composite film, the more DyPW11 particles are aggregated and the rougher of the interface of the composite film.

[1] L. Xu, H. Y. Zhang, E. B. Wang, D. G. Kurth, Z. Li, *J. Mater. Chem*., 2002, **12**, 654.

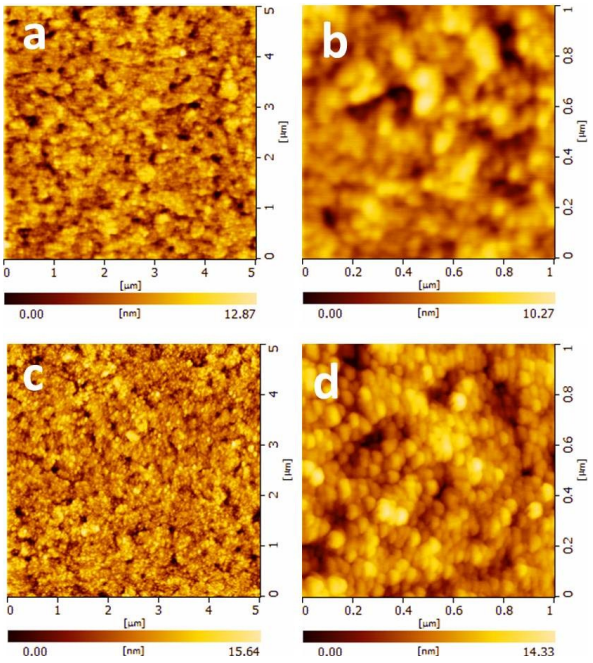

Fig. S12 AFM top images of two composite films $(PEI/DyPW11)_1$ (a, b) and $(PEI/DyPW11)_3$ (c, d) on ITO substrates in the scanning range of 5 μm (a, c) and 1 μm (b, d).

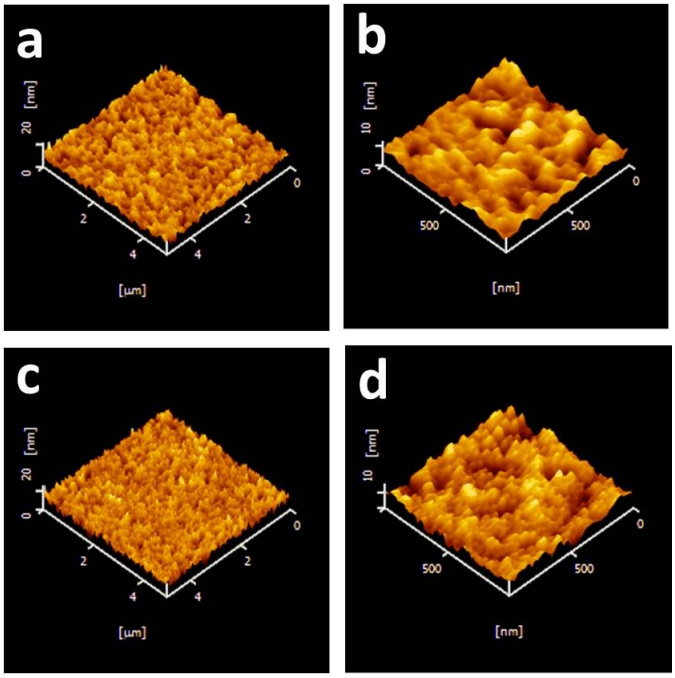

Fig. S13 AFM 3D top images of two composite films $(PEI/DyPW11)_1$ (a, b) and $(PEI/DyPW11)_3$ (c, d) on ITO substrates in the scanning range of 5 µm (a, c) and 1 µm (b, d).

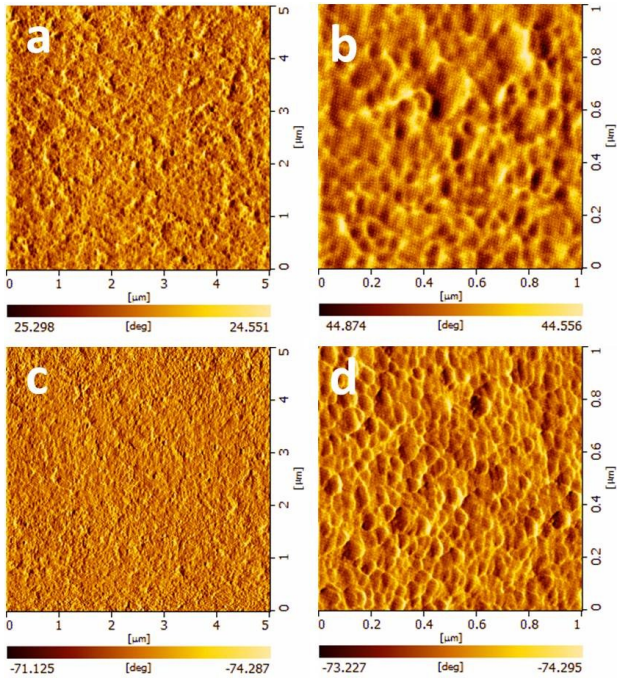

Fig. S14 AFM phase images of two composite films $(PEI/DyPW11)_1$ (a, b) and $(PEI/DyPW11)_3$ (c, d) on ITO substrates in the scanning range of 5 µm (a, c) and 1 µm (b, d).

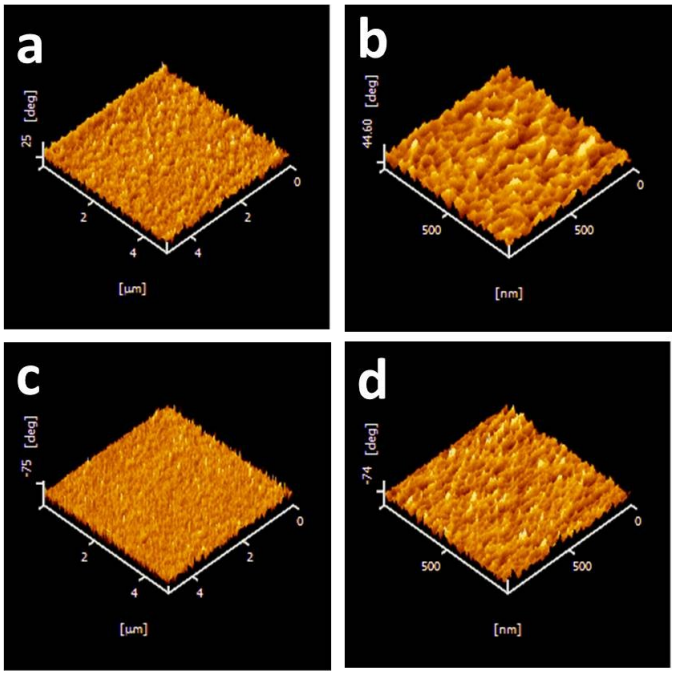

Fig. S15 AFM 3D phase images of two composite films $(PEI/DyPW11)_1$ (a, b) and $(PEI/DyPW11)_3$ (c, d) on ITO substrates in the scanning range of 5 µm (a, c) and 1 µm (b, d).

Table 1. The roughness of two composite films $(PEI/DyPW11)_1$ (a, b) and $(PEI/DyPW11)_3$ (c, d) in the scanning range of 5 µm (a, c) and 1 µm (b, d).

	a	b	c	d
RMS(nm)	1.937	1.64	2.325	2.286
RMS(deg)	0.115	0.05	0.486	0.1657

XPS characterization

XPS spectra of the composite film $(PEI/DyPW11)_{20}$ were measured and the signal peaks of C1s, N1s, O1s, P2p, W4f and Dy4d in the composite film were observed, indicating that DyPW11 is indeed incorporated into the composite film.

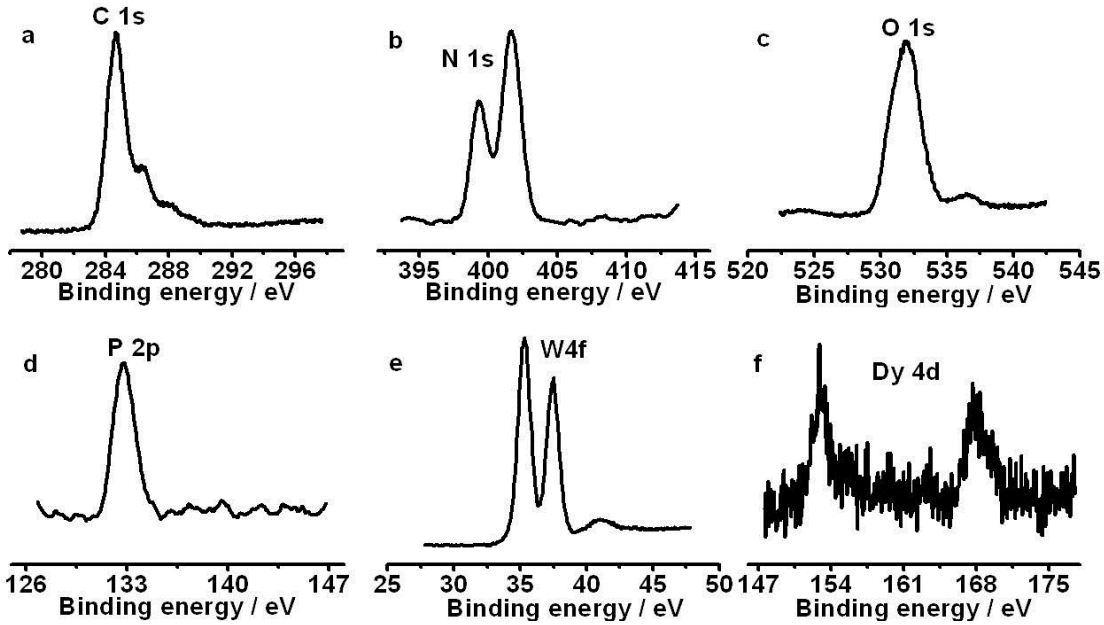

Fig. S16 XPS spectra of the composite film $(PEI/DyPW11)_{20}$.